Journal of Materials Research and Technology 41 (2026) 6963–6969

Contents lists available at ScienceDirect

Journal of Materials Research and Technology

journal homepage: www.elsevier.com/locate/jmrt

Influence of polyvinyl alcohol space holders on the microstructure and porosity of sintered powder metallurgy electrodes

Willian Delfim da Silva [a], Clayton André Oliveira da Motta [a], Lirio Schaeffer [a], Luciano Volcanoglo Biehl [b], José de Souza [b], Jorge Luis Braz Medeiros [b,*]

[a] Federal University of Rio Grande do Sul, Porto Alegre, Rio Grande do Sul, Brazil
[b] Federal University of Rio Grande – FURG, Av. Itália Km 8, Rio Grande, RS, Brazil

ARTICLE INFO

Keywords:
Porous electrodes
Sintered electrodes
Space holder technique
Powder metallurgy

ABSTRACT

Porous metallic electrodes are essential for energy storage and conversion technologies due to their high surface area, enhanced ionic transport, and increased number of electroactive sites. The objective of this study is to investigate the influence of polyvinyl alcohol (PVA) space holders on the microstructure, porosity, and structural connectivity of sintered powder metallurgy iron electrodes, establishing correlations between processing parameters and electrochemical performance. In this study, porous iron electrodes were fabricated via powder metallurgy using polyvinyl alcohol (PVA) as a space holder, aiming to optimize electrochemical performance. The powder mixtures were uniaxially compacted at 60, 80, 100, and 120 MPa, followed by a two step sintering process, with an intermediate step at 300 °C for controlled PVA removal and final sintering at 1050 °C for 30 min under argon with preliminary vacuum. The influence of PVA content on porosity, pore morphology, and microstructural connectivity was systematically evaluated. Morphological analyses showed that PVA promoted the formation of open and interconnected pores, achieving porosity levels that enhance ionic transport and increase the number of electroactive sites compared to conventional powder metallurgy electrodes. Variation in compaction pressure allowed tuning of pore size distribution and densification, enabling a balance between mechanical stability and high porosity. Structural analyses confirmed the stability of the metallic phase and minimal oxidation. These results demonstrate that the PVA space-holder technique enables controlled microstructure design to directly improve electrochemical performance, providing a clear design advantage over conventional electrodes for batteries, fuel cells, and other energy devices.

1. Introduction

In recent years, the transportation sector has increasingly focused on electric vehicles (EVs), which have become a central pillar in the global transition toward sustainable mobility. This transformation is primarily driven by the urgent need to reduce greenhouse gas emissions, particularly CO_2, and to improve overall energy efficiency in response to climate change and growing environmental concerns [1,2]. The electrification of transportation systems represents a strategic pathway to decarbonize road mobility, reduce dependence on fossil fuels, and promote the integration of renewable energy sources into the energy matrix. Consequently, governments, industries, and research institutions worldwide have intensified investments in EVs technologies as part of broader sustainability and carbon neutrality strategies [1,2]. A key factor enabling this transition is the rapid advancement of battery technologies, which directly determine vehicle performance, reliability, and consumer acceptance. Over the past decade, substantial progress in electrochemical systems, materials engineering, and cell design has resulted in significant improvements in energy density, power capability, safety, and cycle life stability. In particular, remarkable reductions in charging times and consistent increases in vehicle driving range have addressed two of the main barriers to large scale EV adoption, namely limited range and long charging durations. Modern battery systems are capable of achieving faster charging rates while maintaining structural and electrochemical stability, thereby reducing the time required to reach high states of charge and enhancing operational convenience [1–4]. In this context, advanced batteries have emerged as one of the most promising solutions, standing out due to their high energy density, long service life, and high operational efficiency. The performance of these devices intrinsically depends on the mechanical

* Corresponding author.
E-mail addresses: willian.delfim@ufgrs.br (W. Delfim da Silva), schaefer@ufrgs.br (L. Schaeffer), jorge.braz@furg.br (J.L.B. Medeiros).

https://doi.org/10.1016/j.jmrt.2026.02.223
Received 1 February 2026; Received in revised form 23 February 2026; Accepted 26 February 2026
Available online 27 February 2026

properties of the materials that make up their electrodes, whose microstructure plays a central role in ionic transport, electronic conduction, and the kinetics of electrochemical reactions [1–4]. The improvement of electrodes, particularly with regard to controlling porosity and internal architecture, has been recognized as one of the main pathways for enhancing battery efficiency and storage capacity. Microstructural analysis including parameters such as total porosity, interconnectivity, tortuosity, and specific surface área makes it possible to simultaneously optimize charge transport and the availability of electroactive sites, elements essential for performance under high-power operation and accelerated charge discharge cycles [3]. In this scenario, porous metal electrodes emerge as particularly attractive candidates, combining high electrical conductivity, low density, large surface area, and adjustable permeability key characteristics for applications that require multifunctional, structurally efficient materials, such as electrochemical devices, catalysts, energy dissipation systems, and lightweight structural components [4,5]. Porous metals constitute a relatively recent class of engineering materials whose structure consists of a continuous solid phase and a network of voids that may exhibit different levels of connectivity [6]. The ability to control the volumetric fraction of pores, along with their size, distribution, and morphology, enables the tuning of material performance for specific requirements, expanding their potential applications in strategic sectors such as sensors, heat exchangers, biomedical implants, electromagnetic shielding, and electrochemical devices [7,8]. Understanding the influence of these structural parameters on properties such as diffusion, permeability, conductivity, and mechanical strength has motivated continuous research efforts, driven by advances in processing and characterization techniques [7,8]. Among the different fabrication routes for porous metallic materials, powder metallurgy (PM) stands out for its versatility, microstructural control potential, and industrial viability [6,7]. PM enables the production of components with complex geometries, adjustable porosity, and customized chemical composition, while also offering advantages such as low material waste, operational simplicity, and reduced costs [9–12]. The combination of mixing, compaction, and sintering steps enables the production of dense, partially dense, or highly porous structures, depending on the parameters adopted, and is widely used to produce metallic electrodes with performance tailored to various operational conditions. The morphology, metallurgical and mechanical properties, and the porosity level of components produced by powder metallurgy are strongly dependent on the sintering temperature and the cooling conditions [13,14]. In particular, the space holder (SH) technique has emerged as an effective strategy for producing highly controlled porous structures. In this approach, temporary particles typically salts, polymers, or hydrides are incorporated into the metal mixture to form voids after their thermal or chemical removal [12]. The method allows precise control of porosity fraction, pore size and shape, and spatial distribution, enabling the fabrication of electrodes with designed architecture, high electrochemically accessible surface area, and low transport losses. The flexibility in choosing the space-forming material, combined with the possibility of using metallic powders with diverse morphologies, further enhances the ability to tailor mechanical, thermal, and electrochemical properties to the specific needs of each device [13]. The electrochemical performance of porous electrodes is strongly influenced by characteristics such as pore network connectivity, tortuosity, and the effective thickness for ion and electron transport 14–16. Thick electrodes can increase areal energy density but often exhibit limitations related to ionic transport, especially at high operating rates, which highlights the importance of microstructural strategies capable of improving the efficiency of active material utilization [15]. Thus, understanding how processing particularly the use of the SH method affects microstructural organization becomes essential for the development of more efficient materials for energy storage. Given this scenario, the present research significant knowledge gaps remain regarding porous metallic electrodes, particularly concerning how microstructure affects ionic and electronic transport during high rate operation, the relationship between processing parameters (such as the space holder method) and the resulting electrochemical and mechanical properties, and the effects of structural degradation over repeated cycles. Additionally, challenges persist in optimizing the trade offs between energy density, transport efficiency, mechanical strength, and production cost, as well as in maintaining uniformity and performance at an industrial scale.

2. Material and methods

The morphology of the samples was investigated by scanning electron microscopy (SEM) using a JEOL® JSM 6510-LV instrument, operating at an accelerating voltage of 20 kV, coupled with a Noran® energy-dispersive X-ray spectroscopy (EDS) system, which allowed the determination of the elemental composition of the sintered samples. Crystallographic analyses were performed by X-ray diffraction (XRD) using a Phillips® X'Pert MPD diffractometer with CuKα radiation and a wavelength of 1.5418 Å. The equipment operated at an accelerating voltage of 40 kV, performing angular scans over a 2θ range of 20° to 80°, with a step size of 0.05° and an acquisition time of 1 s. The diffractograms were processed using the X'Pert HighScore Plus® software, employing data from the Crystallography Open Database (COD) to correlate the identified peaks, enabling the investigation of secondary phase formation during sintering, as well as the assessment of the purity of the metallic matrix.

Vickers microhardness (μHV, HV0.5 kgf) tests were conducted following the recommendations of MPIF Standard 51, specific for the characterization of components manufactured by metal powder processing. Measurements were performed on a Shimadzu® HMV-2000 digital microhardness tester, using a diamond pyramid indenter with a 0.5 kgf load applied for 15 s, in accordance with ASTM E384-17 for material microindentation. Three indentations were made in different regions of each sample, corresponding to the inner, middle, and outer radii, and the mean of the values obtained was used for comparison between conventional samples and those containing PVA as a space holder (SH). The analysis allowed correlating the presence of PVA-induced porosity with the local mechanical strength of the sintered matrix, considering the different compaction pressures investigated.

The main raw material used in this study is water atomized iron powder, commercially designated ASC 100.29 and produced by the Swedish company Höganäs®. This material exhibits chemical purity higher than 99.91%, high compressibility, and particles with predominantly irregular morphology, as shown in the scanning electron microscopy (SEM) image in Fig. 1. The combination of these characteristics favors the powder's compactability, promoting the formation of more homogeneous green compacts. Particle size analysis was conducted by laser diffraction, and the particle size distribution histogram is presented in Fig. 2. The iron powder particles showed diameters ranging from 0.2 to 300 μm, with an average value of 98.64 μm. In the cumulative distribution, it was observed that 10% of the particles have a diameter below 40.22 μm, 50% are at 93.03 μm, and 90% have a diameter below

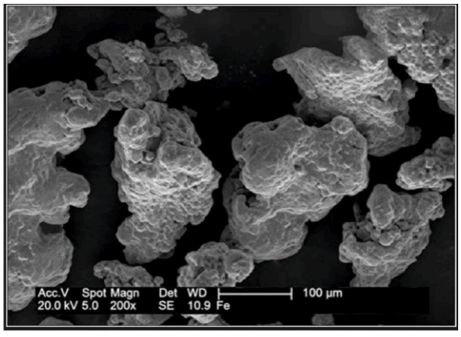

Fig. 1. — ASC 100.29 iron powder particles analyzed by SEM.

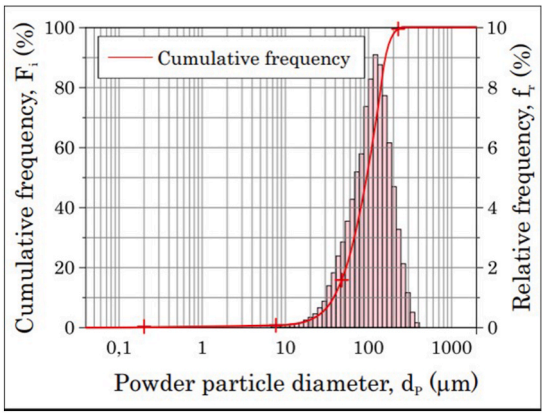

Fig. 2. — Particle size distribution of ASC 100.29 iron powder.

164.31 μm. The apparent density of the material, as reported by the manufacturer, is 2.98 g/cm^3. Polyvinyl alcohol (PVA) powder supplied by the company was used as the space holder (SH).

Neon Analytical Reagents, with an apparent density of 1.27 g/cm^3, whose appearance is shown in Fig. 3. The PVA plays a fundamental role in the process, performing a dual function by initially acting as an organic binder, providing mechanical strength to the green compacts, and later promoting the formation of interconnected pores after its thermal decomposition during the sintering cycle.

The PVA was previously milled in a Retsch® planetary mill, model PM-100, operating at 140 rpm for 15 min with the aim of reducing agglomerates and homogenizing the particle size distribution. After milling, the powder was classified by magnetic agitation using a 100 mesh sieve (approximately 150 μm), removing remaining coarse particles and ensuring a finer and more homogeneous granulometric distribution. Two distinct compositions of metallic powders were prepared. The first consisted of iron powder with the addition of 1 wt% zinc stearate as a lubricant, while the second additionally included 10 wt% PVA. The mixtures were homogenized in a double-cone mixer for 30 min, ensuring uniform dispersion of both the lubricant and the space holder (SH). Powder compaction was carried out in a cylindrical die made of austenitic tool steel AISI D6 with an internal diameter of 13 mm, producing green bodies 3 mm thick, using a Marcon® hydraulic press, model MPH-15, under uniaxial pressures of 60, 80, 100, and 120 MPa. The composition, compaction pressure, and sintering temperature parameters of the samples are presented in Table 1.

The green compacts were sintered in a horizontal resistive muffle furnace manufactured by Sanchis Fornos Industriais®, model Tubular 1600, with prior vacuum and under a positive-pressure atmosphere of pure argon at 0.6 bar and a volumetric flow rate of 2 L/min as carrier gas, in order to minimize oxidation due to the reactivity of the material. The thermal cycle, illustrated in Fig. 4, comprised two stages, using a heating rate of 10 °C/min. The first stage was dedicated to the removal of PVA at 300 °C for 15 min, while the second stage involved iron

Fig. 3. — Sample appearance of the polyvinyl alcohol.

Table 1
Processing parameters of the sintered samples.

Sample identification	**Material composition.**	Compaction pressure, CP[MPa]	Sintering temperature, ϑS [°C]
1	Fe	60	1.050
2	Fe	80	1.050
3	Fe	100	1.050
4	Fe	120	1.050
5	Fe + 10% PVA	60	1.050
6	Fe + 10% PVA	80	1.050
7	Fe + 10% PVA	100	1.050
8	Fe + 10% PVA	120	1.050

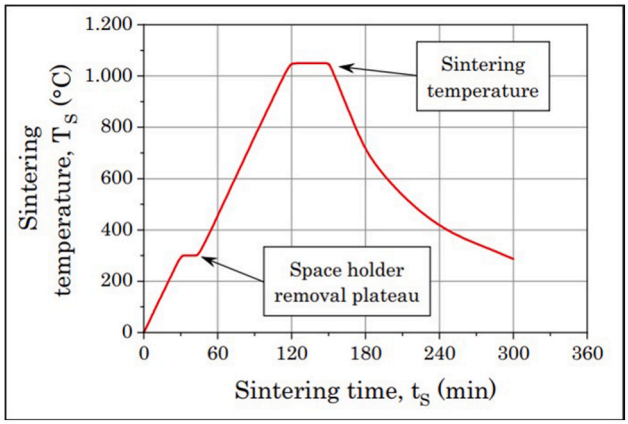

Fig. 4. — Thermal profile of the sintering cycle employed.

sintering at 1050 °C, with a 30 min dwell followed by controlled cooling to room temperature. The physical properties were determined from the absolute density of the sintered samples, ρS (g/cm^3), using Archimedes' principle according to MPIF Standard 42 and ASTM B962-17. The absolute density was calculated using Equation (1), based on the mass and the volume of fluid displaced by the samples when immersed in a liquid of known density.

$$PS = \frac{m_S}{m_S - m_I} PL \quad (1)$$

Where:

ρ_S is the absolute density of the sintered sample, in g/cm^3
m_S it is the dry mass of the sintered material, in g.

m_I is the immersed mass of the sintered sample, in g
ρ_L is the density of the liquid in which the sintered sample is immersed, in g/cm^3

The absolute porosity of the sintered samples, ρ_S (%),was estimated using Equation (2), relating the absolute density to the theoretical density of the material, ρ_T (g/cm^3), which for iron is approximately 7.87 g/cm^3.

$$\phi S = \left(1 - \frac{PS}{PT}\right) 100 \quad (2)$$

Where.

ϕ_S is the absolute porosity of the sintered sample, in %
ρ_S is the absolute density of the sintered sample, in g/cm^3
ρ_T is the theoretical density of the material, in g/cm^3.

3. Results and discussion

3.1. Absolute density

The absolute density of the sintered samples, determined by the Archimedes method, ranged from 4.94 to 6.73 g/cm^3 for the samples obtained by PM, while for those produced by the SH method the values ranged from 3.56 to 4.59 g/cm^3. As shown in Fig. 5, in both processing routes a tendency for the final density to increase with increasing compaction pressure was observed, a behavior associated with the greater packing efficiency of the particles during the compaction stage. However, even under equivalent pressure conditions, the electrodes processed by conventional MP exhibited significantly higher densities than those recorded for the electrodes obtained by the SH method containing 10% PVA [1–10].

The differences observed in the absolute densities obtained by the PM and SH processing methods highlight the intrinsic influence of the manufacturing route on the final microstructure of the sintered electrodes [1,2,12,17]. The higher densities achieved through conventional PM, even under identical compaction conditions, indicate more efficient particle rearrangement and a lower fraction of pores during the green body formation stage. This behavior is expected, since PM directly depends on the consolidation of metallic powder, whereas the SH method incorporates a temporary pore forming agent (PVA), which introduces additional voids that remain after the debinding and sintering stages [1,2,12,17]. Similar trends have been reported in studies involving porous titanium and copper systems, where the addition of space holders systematically reduces packing density and increases overall porosity, even when processed under high compaction pressures. The monotonic increase in density with compaction pressure for both methods reflects the classical densification mechanism, driven by particle deformation, improved interparticle contact, and the reduction of interstitial spaces [1,2,12,17]. However, in materials produced via the SH method, the effect of pressure appears attenuated, suggesting that the compressibility of the powder mixture is restricted by the presence of PVA particles, which act as rigid inclusions during compaction [1,17]. This limitation prevents complete particle rearrangement and reduces the potential densification gain, even when higher compaction pressures are applied. After sintering, the burnout of PVA leaves behind a network of interconnected pores, stabilizing the lower densities observed. Overall, the lower density obtained by the SH method may be desirable depending on the intended application. For electrodes used in electrochemical systems, increased porosity enhances the effective surface area and facilitates electrolyte penetration, potentially improving ion transport and electrochemical performance [5–9]. On the other hand, electrodes produced via MP tend to exhibit greater mechanical stability and lower electrical resistance due to the increased metallic contact between particles [2,12].

3.2. Porosity behavior

Fig. 6 presents the porosity results of the sintered samples. For the samples obtained by conventional powder metallurgy (PM), porosity ranged from 37.2% at a compaction pressure of 60 MPa to 14.6% at 120 MPa. In turn, for those produced using the space holder (SH) method with the addition of PVA, the values ranged from 54.7% to 41.6% at pressures of 60 and 120 MPa, respectively. It can be observed that the samples processed by the SH method exhibited significantly higher porosity compared to those obtained by conventional MP under the same compaction conditions, representing relative increases of 47.0% at 60 MPa and 184.9% at 120 MPa. This behavior confirms the role of PVA as a pore forming agent, whose decomposition and removal during sintering promotes the creation of intentional voids in the metallic matrix, resulting in a substantial reduction in absolute density [5–10]. Thus, the controlled introduction of the pore-forming agent allows modulation of the volumetric fraction of porosity without compromising the overall powder compaction, exerting a direct effect on the microstructure. In summary, although increasing the compaction pressure favors sample densification, the presence of PVA predominantly influences porosity, dimensional stability, and volumetric shrinkage, significantly impacting the sintering and consolidation mechanisms of the material.

The porosity results clearly demonstrate the influence of both the processing route and the compaction pressure on the microstructural characteristics of the sintered samples [1–3,9,10]. Samples produced via the conventional powder metallurgy (PM) method exhibited a significant reduction in porosity with increasing compaction pressure, reflecting the classical densification mechanism in metallic powders, in which higher pressures promote better particle packing and reduce interstitial voids [3,9,10]. This trend is consistent with previous studies on metallic and titanium-based systems, in which densification during compaction is largely governed by particle rearrangement, deformation, and enhanced interparticle contact [18]. In contrast, samples processed using the space holder (SH) method exhibited substantially higher porosity under the same compaction pressures, confirming the role of PVA as an effective pore-forming agent. The decomposition of PVA during sintering introduces additional voids, resulting in a controlled increase in porosity and a concomitant decrease in absolute density. This controlled pore formation is particularly relevant for applications requiring high surface area or fluid permeability, such as electrochemical electrodes or biomedical scaffolds. The relative porosity increase observed at 120 MPa (184.9%) highlights the dominant effect of the pore-forming agent over compaction-induced densification at higher pressures, indicating that the SH method allows for independent tuning of porosity regardless of compaction level. Furthermore, the presence of PVA influences not only porosity but also the dimensional stability and

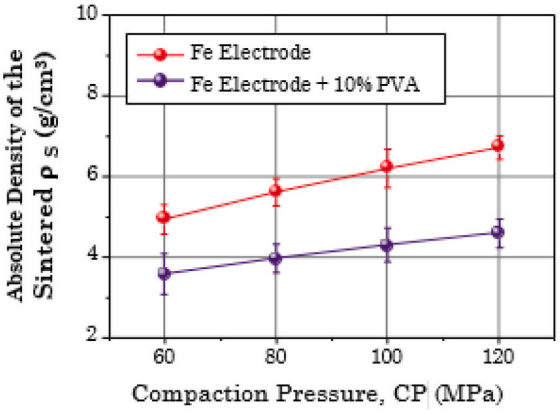

Fig. 5. — Absolute density of the samples as a function of compaction pressure.

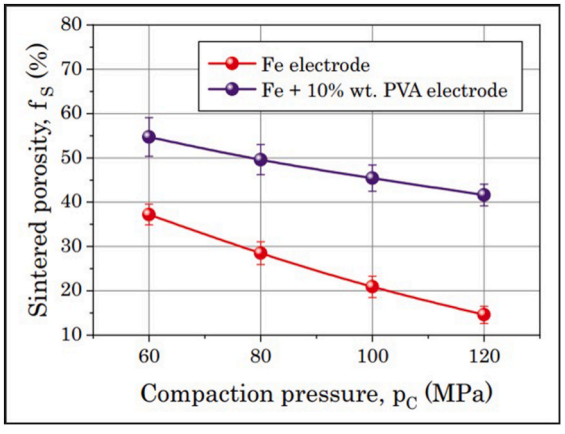

Fig. 6. — Sample porosity as a function of compaction pressure.

volumetric shrinkage of the sintered samples [5–13]. The intentional introduction of interconnected pores can reduce internal stresses during sintering, facilitating the densification of complex geometries, but may also affect mechanical strength. Therefore, while higher compaction pressures are effective in densifying PM samples, in SH samples the microstructure is predominantly determined by the amount, size, and distribution of the pore-forming agent, providing a versatile tool to balance porosity and mechanical performance according to the intended application [3,9,10]. Overall, these results demonstrate that the SH method enables precise control over the volumetric fraction of porosity, offering advantages in designing materials where enhanced permeability or surface area is desired, while MP processing remains preferable when high density and mechanical stability are critical.

3.3. Morphological analyses

The SEM micrographs shown in Fig. 7 reveal marked structural differences between the samples obtained under the different processing conditions.

The sample fabricated by MP exhibits a structure characterized by a predominance of micropores, whose overlap generates interconnected channels, resulting from the packing and sintering of the iron particles. This promotes high surface contact between the particles, enhances the consolidation mechanisms of the structure through neck formation, and increases the active surface area. In contrast, the sample obtained by the SH method displays a dual and hierarchical pore architecture, in which regular macropores, resulting from the removal of PVA particles, are surrounded by cell walls containing a network of micropores, highlighting the role of the spacer in defining the microstructure and in forming a hierarchical porous network [3,5,9,10,13]. The microstructure of sintered electrodes obtained by powder metallurgy (PM) is strongly influenced by the use of polyvinyl alcohol (PVA) as a space holder. Conventional PM samples without PVA exhibit a predominantly microporous structure, where small, irregular pores arise from the natural packing of metal particles. During sintering, the formation of interconnected channels and necks between particles enhances particle consolidation and increases the relative density. In contrast, PM samples prepared with PVA display a dual and hierarchical pore architecture. Regular macropores are generated by the decomposition and removal of PVA particles, while the surrounding cell walls retain a network of micropores formed during sintering 19–21. This hierarchical structure increases the overall porosity and active surface area, resulting in a highly interconnected pore network. The incorporation of PVA as a space holder thus provides an effective strategy to tailor the porosity and microstructural characteristics of sintered electrodes for applications requiring enhanced fluid permeability or surface área [1,3,9,12].

3.4. Analysis by electron microprobe with energy dispersive X ray spectroscopy (EDS)

The sample produced by PM exhibits a structure characterized by the predominance of micropores, whose overlap generates interconnected channels, resulting from the packing and sintering of the iron particles. This promotes high surface contact between particles, facilitates structural consolidation mechanisms through neck formation, and increases the active surface area. In contrast, the sample obtained using the SH method displays a dual and hierarchical pore architecture, in which regular macropores, resulting from the removal of PVA particles, are surrounded by cell walls containing a network of micropores, highlighting the role of the space holder in defining the microstructure and forming a hierarchical porous network. The chemical composition analysis by EDS, shown in Fig. 8, complements the SEM observations by evidencing the main elements present and allowing their distribution to be correlated with the microstructure of the samples. Iron is the predominant element in the samples, with the characteristic Fe-Lα and Fe-Kα peaks confirming the presence of the base metallic matrix, along with the secondary Fe-Kβ line observed in the sample produced by the SH method. The absence of other elements indicates that the integrity of the metallic matrix was not compromised and that the PVA used during processing was completely removed during sintering without leaving residues. In the MP sample, the presence of oxygen was only indicative, suggesting possible superficial oxidation after sintering, likely during handling, but at levels below the detection limit, with no evidence of oxidized phase formation or significant contamination.

3.5. X-ray diffraction (XRD)

The XRD diffractograms presented in Fig. 9 allow the identification of the characteristic peaks of the crystalline phases present in the samples. Small shifts of these peaks relative to crystallographic standards can be attributed to residual stresses induced by the sintering process, without, however, compromising the crystalline structure of the material.

The analysis of the diffractograms revealed that, for both the samples obtained by PM and those produced by the SH method, the main peak at 44.4° is characteristic of the ferritic phase (α-Fe), corresponding to the (110) crystallographic plane of the body-centered cubic (BCC) structure. In both conditions, a secondary peak at 64.7° was also observed, associated with α-Fe and corresponding to the (200) plane. In the sample obtained by MP, additional peaks related to the formation of iron oxides were identified, particularly the presence of magnetite (Fe_3O_4), evidenced by the peaks at 29.8° for the (220) plane, 35.2° for the (311) plane, 56.7° for the (511) plane, and 62.3° for the (440) plane. Furthermore, the occurrence of hematite (α-Fe_2O_3) was verified, indicated by the peak at 32.9° corresponding to the (104) crystallographic plane.(511) e 62,3° de plano (440). Furthermore, the presence of hematite (α-Fe_2O_3) was observed, indicated by the peak at 32.9°

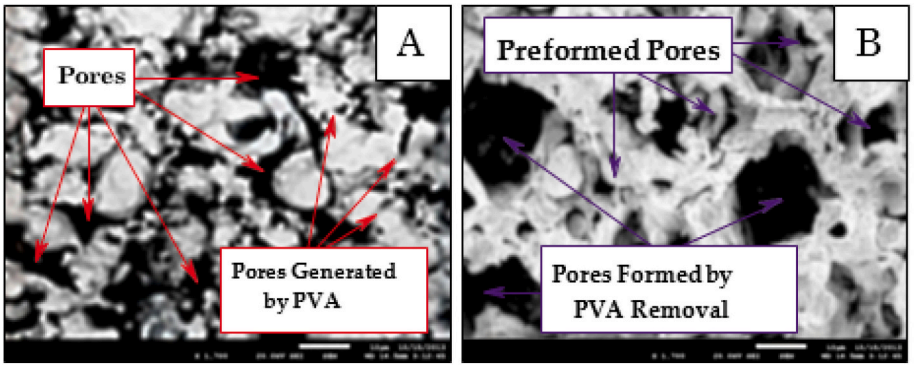

Fig. 7. — Scanning electron microscopy of the electrode samples.A) Sample obtained by PM; B) Sample obtained by the SH method.

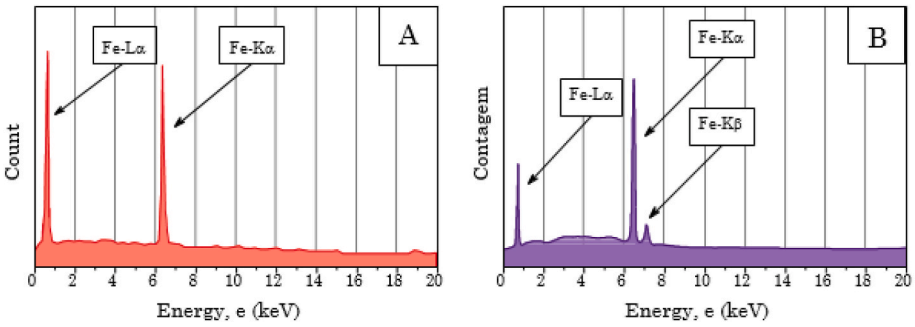

Fig. 8. — Energy-dispersive X-ray spectroscopy (EDS) spectra of the samples.

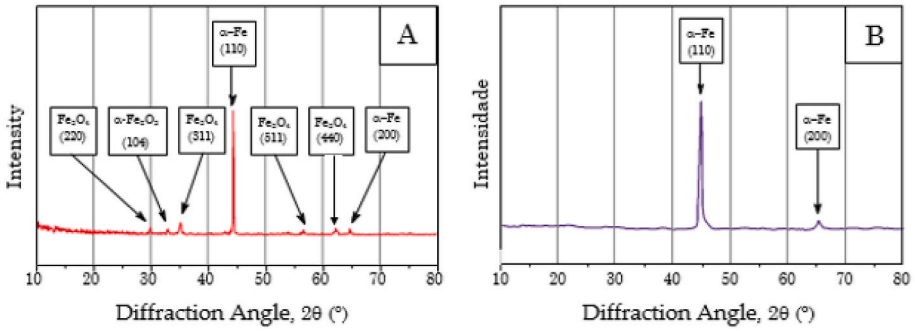

Fig. 9. — A) Sample obtained by MP; B) Sample obtained by the SH method.

corresponding to the (104) crystallographic plane. The formation of oxidized phases in smaller amounts in the samples produced by MP may be associated with superficial oxidation resulting from their removal from the furnace and subsequent exposure to air at temperatures close to 400 °C, a phenomenon reported and influenced by atmosphere conditions and cooling rate [13,17,22].

3.6. Microhardness behavior

The analysis of Vickers microhardness as a function of compaction pressure, presented in Fig. 10, revealed a directly proportional relationship for both processing conditions 18,22–24.

The electrode sample produced by PM exhibited higher microhardness across the entire pressure range, varying from 15.3 to 28.6 HV0.5 kgf for pressures between 60 and 120 MPa. In contrast, the sample obtained by the SH method showed significantly lower values, ranging from 10.1 to 17.7 HV0.5 kgf over the same pressure range. As expected, this difference is attributed to the presence of additional pores introduced by PVA and the distinct consolidation dynamics during sintering, which result in lower density and, consequently, reduced resistance to plastic deformation [6,13,22,24–26]. Furthermore, densification was more effective with increasing compaction pressure, amplifying the difference between the microhardness values obtained by the two methods. These results underscore the importance of densification in enhancing mechanical properties, as higher pressures promote microstructural uniformity and increase resistance to plastic deformation [6,13,24]. The microhardness results clearly demonstrate the strong influence of processing method and compaction pressure on the mechanical performance of the electrode samples. Samples produced via conventional powder metallurgy (PM) exhibited consistently higher microhardness across the entire pressure range, which can be attributed to their higher densification and lower porosity compared to samples produced by the space holder (SH) method. In SH samples, the presence of additional pores introduced by PVA significantly reduces the effective load-bearing area and increases stress concentration points, thereby lowering resistance to plastic deformation and resulting in reduced hardness values. The observed trend of increasing microhardness with higher compaction pressures highlights the critical role of densification in improving mechanical properties. Higher pressures promote better particle rearrangement and interparticle bonding, leading to a more uniform microstructure and enhanced load transfer between particles. This effect is particularly pronounced in PM samples, where the absence of a pore-forming agent allows full densification, whereas in SH samples, even at elevated pressures, the intentional porosity introduced by PVA limits the achievable hardness [3,13,24].

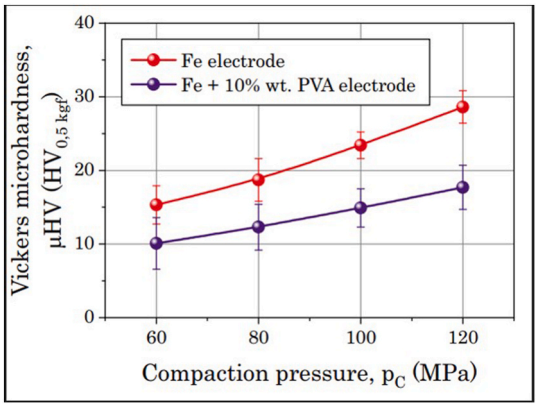

Fig. 10. — Microhardness of the samples as a function of compaction pressure.

4. Conclusion

From the results and discussions, it can be concluded that:

The study of electrodes with controlled porosity has a significant social impact, as it contributes to the development of more efficient energy storage technologies, supports the production of electric vehicles and clean energy systems, and directly reduces CO_2 emissions and the environmental impacts associated with fossil fuel use, thereby

promoting sustainability, energy efficiency, and substantial societal benefits.

The processing strategy has a critical influence on the microstructure, porosity, and mechanical performance of electrodes produced by powder metallurgy (PM) for advanced electrochemical energy storage. Conventional PM electrodes exhibited higher absolute density, lower porosity, and superior hardness, ensuring mechanical stability and dimensional integrity. In contrast, the space holder (SH) method, using PVA as a pore forming agent, enabled precise control over pore size, distribution, and interconnectivity, producing electrodes with lower density and highly tunable hierarchical porosity. This feature is particularly advantageous for battery applications, as it promotes enhanced electrolyte infiltration, improved ionic conductivity, and increased electrochemically active surface area, resulting in higher charge capacity, more efficient charge/discharge kinetics, and superior energy storage performance.

Compaction pressure was shown to modulate densification in both PM and SH electrodes. While higher pressures improved particle packing and hardness in PM samples, SH electrodes maintained substantial porosity due to the PVA template, allowing decoupling of mechanical integrity from functional porosity. Microhardness measurements confirmed this trade off: PM electrodes provide higher load-bearing capacity, whereas SH electrodes optimize pathways for ion transport and electrochemical activity.

These results provide a robust framework for the rational design of metallic battery electrodes via powder metallurgy. By combining controlled pore formation with tailored compaction parameters, electrodes can be engineered to simultaneously achieve high porosity for enhanced ionic and electronic transport and sufficient mechanical stability for long term cycling. The SH approach, in particular, offers a versatile route for next generation batteries, including high power and fast charging systems, where hierarchical porosity and optimized microstructure directly contribute to improved rate performance, energy density, and cycle life. These findings establish clear guidelines for selecting processing routes to meet the stringent demands of advanced electrochemical energy storage devices.

Declaration of competing interest

The authors declare that they have no known competing financial interests or personal relationships that could have appeared to influence the work reported in this paper.

Acknowledgments

The authors acknowledge the support of the Coordination for the Improvement of Higher Education Personnel (CAPES) and the National Council for Scientific and Technological Development (CNPq) for their contribution to scientific funding. This open access publication was enabled and funded by the agreement between the Coordination for the Improvement of Higher Education Personnel (CAPES) and Elsevier, as part of the CAPES Journal Portal.

References

[1] Puška A, Bosna J, Stojanović I. Application of new method evaluation by distance from ideal solution of alternatives in the assessment of electric vehicles. Adv Eng Lett 2025;4(2):92–103.
[2] Dudić B. Global development and sustainability of lithium-ion batteries in electric vehicles. Advanced Engineering Letters 2024;3(2):83–90.
[3] Trung DD, Dudić B, Bao NC, Thinh HX, Duc DV, Ašonja A. Applying probability method for battery electric vehicle selection. 24th international symposium. IEEE; 2025.
[4] Yang Q, et al. Porous electrode materials for Zn-ion batteries: from fabrication and electrochemical application. Batteries, Basel 2022;8(11):223.
[5] Zhou X, et al. A high-performance dual-scale porous electrode for vanadium redox flow batteries. J Power Sources Amsterdam 2016;325:329–36.
[6] Qu D. Fundamental principles of battery design: porous electrodes. In: INTERNATIONAL CONFERENCE OF ELECTROCHEMICAL STORAGE, 1., 2014, Freiberg. *AIP Conference Proceedings*. Melville: American Institute of Physics; 2014. p. 14–25.
[7] Wang Z, et al. Fabrication of three-dimensional porous Cu current collector for lithium-ion batteries using space holder method. Internat J Electrochemical Sci Amsterdam 2021;16(6):1–12.
[8] Dukhan N, et al. Porous metals: from nano to macro. J Mat Res Heidelberg 2020;35 (19):2529–34.
[9] Cui G, et al. Manufacturing of high porosity iron with an ultra-fine microstructure via free pressureless spark plasma sintering. Mat Basel 2016;9(6):495.
[10] Li Y, Dong S, Bai Q, Zhang H, Zhang Q, Li Q. New developments of biomedical porous titanium alloys prepared by spark plasma sintering. Metal Adv 2026;41: 72–84.
[11] Li Y, Bai Q, Dong S, Zhang H, Zhang Q, Li Q, Yang C. Research progress of high porosity biomedical porous titanium alloys. Metals Advances 2026;1:1–31.
[12] Ayub H, et al. Investigating the morphology, hardness, and porosity of copper filters produced via hydraulic pressing. Journal of Materials Research and Technology, Amsterdam 2022;19:208–19.
[13] Sutrisna S, Purnomo MJ, Wartono W, Prasetiyo AB, Riadji MIS, Mingwaro WP. Optimisation of microstructure and wear properties of porous Fe-Cu bearing materials. Tribology and Materials 2026;1:1–13.
[14] Kumar P, Srivastava VK, Sharma A. Influence of cooling mediums on mechanical and tribological characteristics of Al/Cu-based composites reinforced with chromium particles. Tribology and Materials 2025;4(3):134–43.
[15] Jang ES, Kang CW. An experimental study on pore structural changes of ultrasonic treated Korean paulownia (*Paulownia coreana*). Wood Science and Technology, New York 2022;56(3):883–98.
[16] Santhanagopalan S, White RE. Porous electrodes. In: GARCHE J, editor. Encyclopedia of electrochemical power sources. Amsterdam: Elsevier; 2009. p. 110–20.
[17] a Bai Y, et al. Preparation of graphene–carbonyl iron poder tri-iron tetroxide composite and its better microwave absorption properties. J Mater Sci: Materials in Electronics, Dordrecht 2019;30:5454–63.b Zhang Y, Wu S, Guo Z, Peng G, Wang L, Yan W. Defects caused by powder spattering and entrainment in laser powder bed fusion process: High-fidelity modeling of gas, melt pool and powder dynamics. Acta Mater 2025;288:1–15.
[18] Yanping H, et al. Effects of the space holder size on the pore structure and mechanical properties of porous Cu with a wide porosity range. Scientific Reports, Berlin 2025;15(1):11072.
[19] a Bętkowska A, et al. Microstructure and mechanical properties of highly porous Hastelloy-X nickel superalloy produced by a space holder approach. Scientific Reports, Berlin 2025;15(1):598.b Cavilha Neto F, Giaretton MV, Neves GO, Aguilar C, Souza MT, Binder C, Klein AN. An overview of highly porous titanium processed via metal injection molding in combination with the space holder method. Metals 2022;12:1–21.
[20] Gonçalves AHA, et al. Synthesis of a magnetic Fe_3O_4/RGO composite for the rapid photo-fenton discoloration of indigo carmine dye. Topics in Catalysis, New York 2020;63:1017–29.
[21] Medeiros JLB, Martins COD, Biehl LV. Effect of sintering atmosphere control on the surface engineering of Catamold steels produced by MIM: a review. Surfaces 2025; 9:1–18.
[22] Medeiros JLB, Biehl LV, Martins COD, Pacheco DADJ, Souza J, Reguly A. Assessment of residual stress behavior and material properties in steels produced via oxynitrocarburized metal injection molding. J Mater Eng Perform 2024;33: 1–11.
[23] Zhang Q, Yi B, Liu R, Peng X. Topology optimization of porous electrodes for enhanced mass transport and electrochemical performance. Chem Eng J 2026;528: 1–15.
[24] Palliyarayil A, Vinayakumar K, Shunmuga Kumar N, Sil S. Porous activated carbon from nitrogen rich pulses: harnessing naturally occurring nitrogen for enhanced CO_2 capture. Biomass Bioenergy 2026;208:1–15.
[25] Tocchetto R, et al. Evaluations of the space holders technique applied in powder metallurgy process in the use of titanium as biomaterial. Lat Am Appl Res 2019;49: 261–8.
[26] Das Neves EC, et al. Nondestructive analysis of corrosion in ageing hardened AA6351 aluminium alloys. Mater Chem Phys 2022;291:126664–93.